Structural Monitoring and Maintenance, *Vol. 8, No. 4 (2021) 329-344*
https://doi.org/10.12989/smm.2021.8.4.329

Configuration assessment of MR dampers for structural control using performance-based passive control strategies

Zubair R. Wani [1a], Manzoor A. Tantray [1b], Javed Iqbal [2c] and Ehsan Noroozinejad Farsangi*[3,4,5,6]

[1] *Department of Civil Engineering, National Institute of Technology Srinagar, India*
[2] *Department of Electrical Engineering, National Institute of Technology Srinagar, India*
[3] *Faculty of Civil and Surveying Engineering, Graduate University of Advanced Technology, Kerman, Iran*
[4] *School of Civil Engineering and the Built Environment, University of Johannesburg, Johannesburg, South Africa*
[5] *International Institute for Urban Systems Engineering (IIUSE), Southeast University, Nanjing, China*
[6] *Smart Structures Research Group, The University of British Columbia, Vancouver, Canada*

(*Received April 22, 2021, Revised August 14, 2021, Accepted September 29, 2021*)

Abstract. The use of structural control devices to minimize structural response to seismic/dynamic excitations has attracted increased attention in recent years. The use of magnetorheological (MR) dampers as a control device have captured the attention of researchers in this field due to its flexibility, adaptability, easy control, and low power requirement compared to other control devices. However, little attention has been paid to the effect of configuration and number of dampers installed in a structure on responses reduction. This study assesses the control of a five-story structure using one and two MR dampers at different stories to determine the optimal damper positions and configurations based on performance indices. This paper also addresses the fail-safe current value to be applied to the MR damper at each floor in the event of feedback or control failure. The model is mathematically simulated in SIMULINK/MATLAB environment. Linear control strategies for current at 0 A, 0.5 A, 1 A, 1.5 A, 2 A, and 2.5 A are implemented for MR dampers, and the response of the structure to these control strategies for different configurations of dampers is compared with the uncontrolled structure. Based on the performance indices, it was concluded that the dampers should be positioned starting from the ground floor, then the 2nd floor followed by 1st and rest of the floors sequentially. The failsafe value of current for MR dampers located in lower floors (G+1) should be kept at a higher value compared to dampers at top floors for effective passive control of multi-story structures.

Keywords: configuration; linear control; MR damper; performance index; structural dynamics; structural response

1. Introduction

In recent years' there has been an upsurge in research field of semi-active structural control to overcome structural limitations during a seismic event (Basu *et al*. 2014). Various control devices

*Corresponding author, Ph.D., Assistant Professor, E-mail: noroozinejad@kgut.ac.ir
[a] Ph.D. Candidate
[b] Professor
[c] Associate Professor

http://www.techno-press.org/?journal=smm&subpage=7 ISSN: 2288-6605 (Print), 2288-6613 (Online)

have been developed and implemented till date such as passive, active and semi-active devices. The passive control system does not require any external power source and uses structural motion to dissipate kinetic energy or isolate the vibration so that the response can be controlled passive (He *et al*. 2016a, b, Aydin *et al*. 2019a, b, Cetin *et al*. 2019). In Active control, a large external source of energy is used to activate the control system by providing a control signal to an actuator (Hagood *et al*. 1990, Spencer and Nagarajaiah 2003, Stanway 2004, Korkmaz 2011, Preumont 2011). In semi-active devices, external power is only used to change the device's properties such as damping or stiffness, and not to generate a control force. Hence, the power requirement is very low (Poynor 2001, Çeşmeci and Engin 2010, Berasategui *et al*. 2014, Wani and Tantray 2020).

From the semi-active control devices available in the market, Magnetorheological (MR) dampers are considered most reliable, for its flexibility and adaptability. As the cost of the MR dampers for an actual structure is substantial, therefore installing MR damper on each floor of structure is uneconomical. To achieve effective structural control, it is of paramount importance to determine the optimal position and configuration of limited number of semi active control devices. The performance-based model is a viable and effective optimization method. An algorithm for the placement procedure of MR damper is proposed such that the peak inter-story drifts, displacement and acceleration would be restricted to a quantified value (Lindberg and Longman 1984, Ibidapo-Obe 1985, Dhingra and Lee 1994, Abdullah *et al*. 2001, Xu and Teng 2002, Cimellaro 2012). The performance-based procedure design takes into consideration the non-linear behavior of MR dampers for varying input current and the non-classical damping of the structure (Chen *et al*. 2010, 2018, Chaudhury and Singh 2014, Zhou *et al*. 2018, Nabid *et al*. 2019). The performance level of the structure, which intern indicates the permissible damages to the structure, can be selected by the designer. Depending on the type of the structure in consideration, some performance indices require more stringent consideration and hence can take primary preference in performance-based design, which can be reduced by adding more energy dissipation devices than required (Singh and Moreschi 2002, Yanik 2020).

As the cost of the MR dampers for an actual structure is substantial, therefore installing MR damper on each floor of structure is uneconomical. In order to achieve effective structural control, it is of paramount importance to determine the optimal position and configuration of a limited number of semi-active control devices. The performance-based model is a viable and fairly effective optimization method. An algorithm for the placement procedure of MR damper is proposed such that the peak inter-story drifts, displacement and acceleration would be restricted to a quantified value (Yoshida and Dyke 2005, Wani and Tantray 2021). The performance-based procedure design takes into consideration the non-linear behavior of MR dampers for varying input current and the non-classical damping of the structure (Wani and Tantray 2021). The performance level of the structure which intern indicates the permissible damages to the structure can be selected by the designer. Depending on type of the structure in consideration, some performance indices require more stringent consideration and hence can take primary preference in performance-based design which can be impeded by adding more energy dissipation devices than required. Previous studies involve empirical approach to determine the optimal placement and configuration of dampers (Qiu *et al*. 2007). Zhang *et al*. (2018) proposed an extended method based on sequential addition of dampers to obtain maximum reduction in inter-story drift. Search technique was adopted by Agrawal *et al*. (1998) to determine the prime placement of structural control devices.

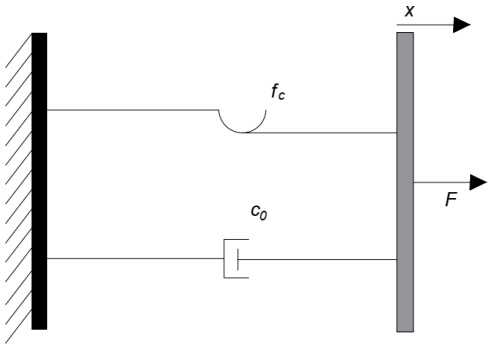

Fig. 1 Bingham model for MR dampers

2. Mathematical model of MR damper

Many mathematical models have been proposed to efficiently describe the behavior of MR damper (Jolly *et al*. 1999, De Vicente *et al*. 2011, Guan *et al*. 2011, Spaggiari 2012) for use in time history and random vibration analyses. One of the common models used is the Bingham model for MR dampers which is comprised of a viscous element and a frictional element (Hong *et al*. 2008). The schema Bingham of the model is illustrated in Fig. 1. The force generated by the MR dampers is given by Eq. (1)

$$F(t) = c_0\dot{x}(t) + f_c\, sgn\,[\dot{x}(t)] + f_0 \tag{1}$$

Where c_0 is the damping coefficient, $\dot{x}$(t) is the velocity response of the damper to external excitation, c_0 is the damping coefficient, f_c is the frictional force depending upon the input current and field-dependent yield stress and f_0 is the force included to account for the nonzero mean observed in the measured force due to the presence of the accumulator.

Also

$$f_c = \frac{3L_dA_p\tau_y}{h_d} \quad \text{and} \quad c_0 = \frac{12L_dA_p{}^2}{\pi D h_d{}^3}$$

where h_d is the gap between the piston and the cylinder, *Ld* is the length of the piston, A_p is the cross-sectional area of the piston, *D* is the inner diameter of the cylinder, h_d is the gap between the piston and the cylinder, $x(t)$ is the relative displacement of the piston to the cylinder, and τ_y is the function of the current I_c (applied magnetic field). The relation between τ_y and current I_c for MR damper was established as shown in Eq. (2).

$$\tau_y = A_1e^{-I_c} + A_2\ln(I_c + e) + A_3I_c \tag{2}$$

Where e is a constant. A_1, A_2 and A_3 are coefficients relative to the property of MR fluid in the MR damper.

The MR damper to be used in this particular research is a 200 KN valve type damper where the input current can be varied from 0-3 A. The parameters of the damper are shown in Table 1. The damper is modeled using the above equations. In order to depict the behavior and energy

Table 1 Parameters of MR damper

Stroke (mm)	±50
External diameter (mm)	194
Internal diameter (mm)	160
Diameter of Piston (mm)	80
Effective length of piston (mm)	250
Damping Gap (mm)	2

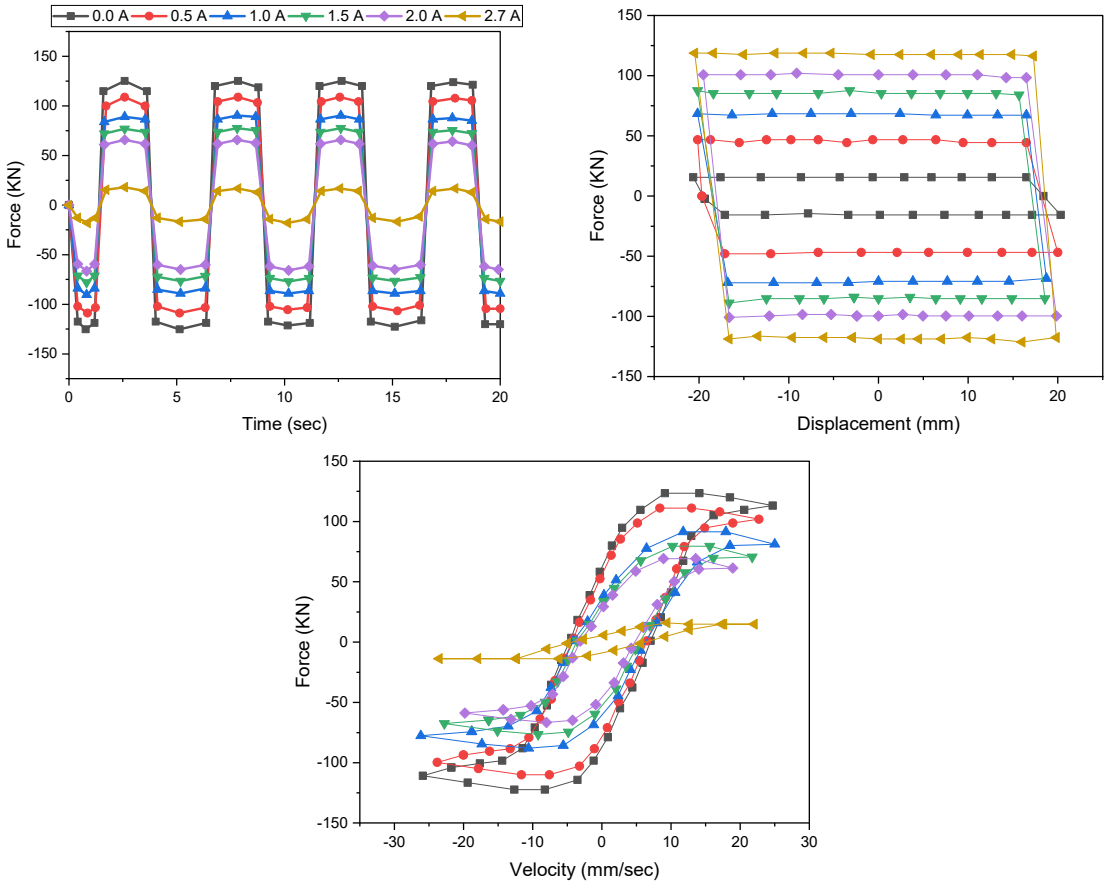

Fig. 2 Hysteresis curves of Force (N) vs time, Force (N) vs displacement and Force (N) vs velocity for MR damper subjected to sinusoidal excitation of amplitude 20 mm and frequency of 0.2 Hz

dissipation characteristics of MR damper, it is subjected to sinusoidal excitation of varying amplitudes and frequency for different input current. Fig. 3 shows hysteresis curves of force vs time, force vs displacement and force vs velocity for MR damper subjected to sinusoidal excitation of amplitude 20 mm and frequency of 0.2 Hz. The input currents are taken as 0 A, 0.5 A, 1 A, 1.5 A, 2 A and 2.7 A.

3. Mathematical model of Structure with MR damper

The five-story steel structure in consideration in this study which is taken from the book published by Xu *et al*. (2016). The height of each column is 3.3 m and the length of each beam is 5 m. The mathematical equation for the model of a structure with a control device subjected to a dynamic excitation is given in Eq. (3).

$$[\boldsymbol{M}]\{\ddot{x}(t)\} + [\boldsymbol{C}]\{\dot{x}(t)\} + [\boldsymbol{K}]\{x(t)\} = \{P(t)\} + [\boldsymbol{B}]\{f(t)\} \tag{3}$$

where $\{\ddot{x}(t)\}$, $\{\dot{x}(t)\}$ and $\{x(t)\}$ are acceleration, velocity and displacement response vectors respectively. Also **[M]**, **[C]** and **[K]** are mass, damping and stiffness square matrices for the structure. {P(t)} can be any external excitation i.e., earthquake or wind load. {f(t)} is the control force generated by the control device installed in the structure and [B] is its position matrix. The lumped mass matrix **[M]** for the structure in consideration is taken as

$$M = \begin{bmatrix} 2.60 & 0 & 0 & 0 & 0 \\ 0 & 2.30 & 0 & 0 & 0 \\ 0 & 0 & 2.30 & 0 & 0 \\ 0 & 0 & 0 & 2.30 & 0 \\ 0 & 0 & 0 & 0 & 2.00 \end{bmatrix} \times 10^4 \text{ kg}$$

The structural stiffness matrix **[K]** is taken as

$$K = \begin{bmatrix} 4.38 & -2.32 & 0 & 0 & 0 \\ -2.32 & 4.64 & -2.32 & 0 & 0 \\ 0 & -2.32 & 4.64 & -2.32 & 0 \\ 0 & 0 & -2.32 & 4.64 & -2.32 \\ 0 & 0 & 0 & -2.32 & 2.32 \end{bmatrix} \times 10^7 \text{ N/m}$$

And damping matrix **[C]** is calculated in accordance with the most popular Rayleigh damping hypothesis.

$$C = \begin{bmatrix} 2.15 & -1.06 & 0 & 0 & 0 \\ -1.06 & 2.25 & -1.06 & 0 & 0 \\ 0 & -1.06 & 2.25 & -1.06 & 0 \\ 0 & 0 & -1.06 & 2.25 & -1.06 \\ 0 & 0 & 0 & -1.06 & 1.17 \end{bmatrix} \times 10^5 \text{ N} - \text{s/m}$$

$$[\mathbf{M}]\{\ddot{x}(t)\} + [\mathbf{C}]\{\dot{x}(t)\} + [\mathbf{K}]\{x(t)\} = -[\mathbf{M}]\{\Gamma\}\ddot{x_g}(t) + [\mathbf{B}]\{f(t)\} \tag{4}$$

where $\{\Gamma\} = \{1,1,\dots,1\}^T$ is a column vector and $\ddot{x_g}$(t) is the acceleration of earthquake excitation. The above Eq. (5) can be rewritten as the state space equation as

$$\begin{aligned} \{\dot{Z}(t)\} &= [\mathbf{A}]\{Z(t)\} - [D_0]P(t) + \{L\}[G]\{f(t)\} \\ \{Y\} &= [E_0][Z(t)] \end{aligned} \tag{5}$$

Where {Y} is the output vector and {Z(t)} is the state vector of displacement and velocity: and $[A] = \begin{bmatrix} [0] & [I] \\ -[M]^{-1}\,[K] & -[M]^{-1}\,[C] \end{bmatrix}$ is the structural system matrix. $[D_0] = \begin{bmatrix} [0] \\ [M]^{-1} \end{bmatrix}$; $[G]$

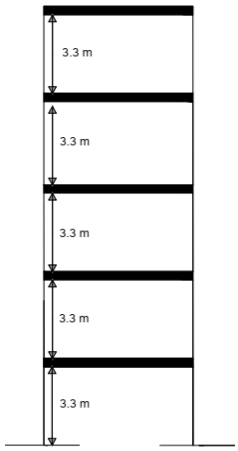

Fig. 3 Five storied framed structure

$\begin{bmatrix} [0] \\ [M]^{-1}B \end{bmatrix}$ is the input matrix; {L} is the vector corresponding to the position of damper and [E0] = [[I] [0]] is the output matrix to obtain the required structural responses, where [I] is the identity matrix and [0] is the null matrix.

3.1 Model configuration

The MR dampers are placed parallel to the floor for different configurations and numbers in Chevron brace arrangement. According to the configuration and position of dampers, models are categorized as ***M*** and ***N for*** 1 and 2 MR dampers installed as shown in Figs. 4(a) and 4(b), respectively. The structural response of each model subjected to 100-gal El-Centro excitations is obtained. {L} matrix for each model used in MATLAB/SIMULINK is stated in Table 1.

3.2 Seismic ground motion considered

A total of 10 seismic ground motions are used to determine the efficiency and performance of passive control devices employing multiple dampers is MATLAB/Simulink. The accelerograms in consideration are downloaded from the PEER ground motion database by the University of Berkeley (Peer 2013). The unscaled seismic records chosen involve (1) Imperial Valley (El Centro) caused by strike-slip mechanism, (2) Kobe_ABN earthquake with fault parallel component, (3) North California earthquake caused by the normal strike, (4) Northridge_ANA earthquake

Table 2 Position of the damper in the model

Position of the single damper	Matrix {L}	Position of two dampers	Matrix {L}
Ground floor	$\{L\}_{M1} = [1\ 0\ 0\ 0\ 0]^T$	Both in ground floor	$\{L\}_{N1} = [2\ 0\ 0\ 0\ 0]^T$
Between ground and 1st floor	$\{L\}_{M2} = [0\ 1\ 0\ 0\ 0]^T$	One ground and other in 1st	$\{L\}_{N2} = [1\ 1\ 0\ 0\ 0]^T$
Between 1st and 2nd floor	$\{L\}_{M3} = [0\ 0\ 1\ 0\ 0]^T$	One ground and other in 2nd	$\{L\}_{N3} = [1\ 0\ 1\ 0\ 0]^T$
Between 2nd and 3rd floor	$\{L\}_{M4} = [0\ 0\ 0\ 1\ 0]^T$	One ground and other in 3rd	$\{L\}_{N4} = [1\ 0\ 0\ 1\ 0]^T$
Between 3rd and 4th floor	$\{L\}_{M5} = [0\ 0\ 0\ 0\ 1]^T$		

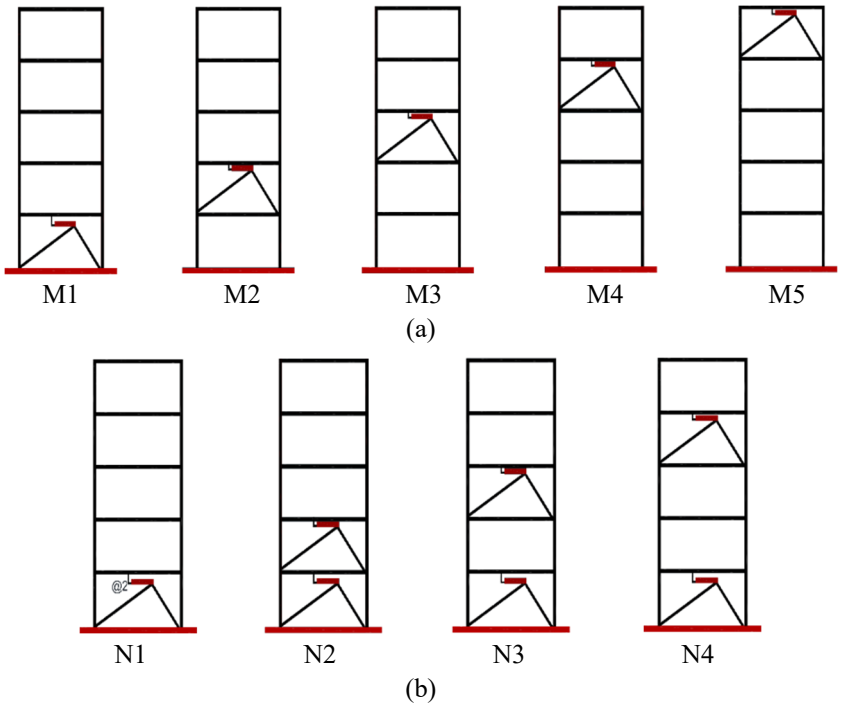

Fig. 4 M-type models with 1 MR damper and N-type models with 2 MR damper

(Castaic-Old Ridge Route) caused by reverse slip mechanism and (5) Friuli Italy-01 caused by a strike-slip mechanism. The details of the selected time history records are tabulated in Table 2. The records are chosen in such a way that they cover as wide intensity, frequency, and velocity range as possible. Another factor taken into consideration when selecting input excitation is that the maximum horizontal first-floor displacement does not exceed the damper stroke limit.

3.3 Linear control strategy and Performance index

Linear control of structure involves passive on and off condition of MR dampers for previously mentioned models. The maximum structural responses of 5th, 3rd and 1st floor for each model were subjected to different intensity of ground motions for the value of input current to the damper set at 0 A, 0.5 A, 1 A, 1.5 A, 2 A and 2.5 A are obtained and tabulated under. Table 3 shows the maximum responses of uncontrolled structure, Tables 4-8 and Tables 9-12 show the maximum acceleration, displacement and inter-story drift responses for models ***M*** and ***N*,** respectively.

The performance indices (***PI***) for models are considered corresponding to: (1) maximum reduction in floor displacement; (2) maximum reduction in floor acceleration; and (3) maximum reduction in inter-story drift. The performance indices for each model of ***M*** and ***N*** are obtained based on the minimum value obtained for the average square root of the sum of squares of all floors for each linear control strategy.

$$\boldsymbol{PI}_{displ} = \frac{1}{N}\sqrt{\sum_{1}^{i}\left(u_i^2\right)}, \quad \boldsymbol{PI}_{displ} = \frac{1}{N}\sqrt{\sum_{1}^{i}\left(a_i^2\right)}, \quad \text{and} \quad \boldsymbol{PI}_{displ} = \frac{1}{N}\sqrt{\sum_{1}^{i}\left(d_i^2\right)}$$

Table 3 Seismic ground motion considered in this study

S No.	Earthquake record	Year	Recording station	PGA (m/sec^2)
1	Kobe (Japan)	1995	Nishi	4.530
2	Imperial valley (California)	1940	El-Centro array #9	3.104
3	Northern Calif (USA)	1954	Ferndale City Hall	1.632
4	Northridge (Los Angeles)	1994	Lake Hughes #12A	0.943
5	Friuli (Italy)	1976	Cordeiro	0.687
6	S Fern	1971	Hawaii, USA	0.981
7	Chi Chi	1999	Taiwan	0.197
8	Big Bear	1992	California, USA	0.343
9	Dinar	1995	Turkey	0.392
10	Kozani	1995	Greece	0.235

Where u_i, a_i and d_i are maximum floor displacement, acceleration and interstory drift of i^{th} floor where i vary from 1 to 5 and N = 5

The process of obtaining optimal configuration of MR damper is illustrated below:

For M type model: Single MR damper is first installed at the ground floor of the structure (M1) and subjected to different set of seismic excitations and passive on controller (0 A to 2.5 A). The MR damper is moved to 1st floor (M2) and structural response corresponding to different passive control and seismic excitations are obtained. Similarly, structural responses corresponding to different positions of MR damper from ground to top floor are compared to obtain the optimal position of a single MR damper.

The optimal placement of MR damper and particular passive control (value of input current) are ascertained based on performance index i.e., maximum attenuation of Acceleration, displacement and inter-story drift responses.

For N type model:

As the optimal position for single MR damper is ascertained at the ground floor, for N-type models the position of 2nd MR damper is altered. Firstly, Both MR dampers are placed in the ground floor (N1) and the structure is subjected to different seismic excitations for varying input current (0 to 2.5 A). Next, the MR damper is moved to the first floor keeping the damper at ground floor fixed (N2) and response of structure to different seismic excitation are recorded. Similarly, response corresponding to configuration N3 and N4 are recorded.

The optimal configuration of 2 MR dampers and their corresponding passive control settings are determined from comparing and contrasting the performance indices.

Table 4 Maximum response of uncontrolled structure

Floor	Displacement (m)	Acceleration (m/sec^2)	Inter-story drift (m)
5th	0.050431	5.434501	0.004663
3rd	0.037151	3.642371	0.010791
1st	0.015601	1.758188	0.015601

Table 5 Maximum response for model M1

Floor	Current	Displacement	Acceleration	Inter-story drift	Current	Displacement	Acceleration	Inter-story drift
5th		0.044133	3.594585	0.004473		0.029534	2.991981	0.010434
3rd	**0 A**	0.035236	3.524865	0.010270	**1.5 A**	0.008689	3.017378	0.000005
1st		0.014727	1.639051	0.014727		0.008689	5.288276	0.008689
5th		0.034565	3.423428	0.005497		0.029169	3.156805	0.004367
3rd	**0.5 A**	0.027149	3.28959	0.008213	**2 A**	0.023489	3.156805	0.007564
1st		0.010710	2.381966	0.010710		0.00835	6.288205	0.008350
5th		0.030508	3.102675	0.003407		0.02906	3.455334	0.002901
3rd	**1 A**	0.024022	3.03205	0.008377	**2.5 A**	0.023576	2.910298	0.008670
1st		0.009195	4.012927	0.009195		0.008071	7.035184	0.008071

Table 6 Maximum response for model M2

Floor	Current	Displacement	Acceleration	Inter-story	Current	Displacement	Acceleration	Inter-story
5th		0.04451	3.652506	0.004480		0.040764	9.555597	0.003614
3rd	**0 A**	0.03560	3.58928	0.010316	**1.5 A**	0.033581	10.661	0.007980
1st		0.014999	1.756053	0.014999		0.017652	13.74868	0.017652
5th		0.038014	5.058185	0.005654		0.042325	10.80794	0.006282
3rd	**0.5 A**	0.030689	5.348701	0.008696	**2 A**	0.034197	11.94713	0.007718
1st		0.013282	6.770942	0.013282		0.018741	15.69216	0.018741
5th		0.038009	7.908908	0.003293		0.043182	11.71749	0.004681
3rd	**1 A**	0.031844	8.852295	0.010413	**2.5 A**	0.034286	12.81908	0.008970
1st		0.013657	11.13317	0.013657		0.019463	17.19661	0.019463

Table 7 Maximum response for model M3

Floor	Current	Displacement	Acceleration	Inter-story	Current	Displacement	Acceleration	Inter-story
5th		0.044711	3.686503	0.004419		0.04371	8.717255	0.003887
3rd	**0 A**	0.035923	3.600005	0.010378	**1.5 A**	0.035984	9.223246	0.007322
1st		0.015199	1.903009	0.015199		0.021376	8.872884	0.021376
5th		0.040091	5.047032	0.005970		0.044441	10.10383	0.006022
3rd	**0.5 A**	0.032351	5.094975	0.008508	**2 A**	0.037126	10.30088	0.007164
1st		0.015318	3.809384	0.015318		0.022777	9.356945	0.022777
5th		0.042848	7.000867	0.004518		0.045022	11.1287	0.003782
3rd	**1 A**	0.034277	7.808685	0.008973	**2.5 A**	0.037958	10.99261	0.008818
1st		0.019447	6.907564	0.019447		0.02391	9.802641	0.023910

Table 8 Maximum response for model M4

Floor	Current	Displacement	Acceleration	Inter-story	Current	Displacement	Acceleration	Inter-story
5th		0.045141	3.673828	0.004434		0.056768	13.14853	0.010831
3rd	**0 A**	0.036323	3.64451	0.010507	**1.5 A**	0.035162	12.14968	0.005260
1st		0.015341	1.895989	0.015341		0.024679	10.48823	0.024679
5th		0.049008	7.568656	0.010458		0.059305	14.94427	0.014209
3rd	**0.5 A**	0.032838	6.559034	0.008367	**2 A**	0.036438	13.77705	0.004694
1st		0.016086	5.044419	0.016086		0.027027	12.10161	0.027027
5th		0.053478	10.80567	0.010324		0.061339	16.38564	0.012154
3rd	**1 A**	0.033353	10.03143	0.007514	**2.5 A**	0.037627	15.28752	0.006216
1st		0.021506	8.364944	0.021506		0.029062	13.41214	0.029062

Table 9 Maximum response for model M5

Floor	Current	Displacement	Acceleration	Inter-story	Current	Displacement	Acceleration	Inter-story
5th		0.045779	3.679545	0.004531		0.046401	15.91022	0.004733
3rd	**0 A**	0.036768	3.625397	0.010665	**1.5 A**	0.036986	7.587326	0.007345
1st		0.01547	1.804477	0.015470		0.022332	7.760309	0.022332
5th		0.04368	6.492348	0.006766		0.048739	17.43878	0.007796
3rd	**0.5 A**	0.034692	3.94972	0.009966	**2 A**	0.038188	7.964507	0.007020
1st		0.014743	3.813978	0.014743		0.024125	8.86363	0.024125
5th		0.045783	13.20107	0.005253		0.050566	18.82691	0.006084
3rd	**1 A**	0.035768	6.818156	0.010094	**2.5 A**	0.038938	8.358515	0.008648
1st		0.01874	5.674711	0.018740		0.025372	9.599359	0.025372

Table 10 Maximum response for model N1

Floor	Current	Displacement	Acceleration	Inter-story	Current	Displacement	Acceleration	Inter-story
5th		0.0397197	3.378909	0.004026		0.0265806	2.812462	0.009391
3rd	**0 A**	0.0317124	3.313373	0.009243	**1.5 A**	0.0078201	2.836335	0.000005
1st		0.0132543	1.540707	0.013254		0.0078201	4.970979	0.007820
5th		0.0311085	3.218022	0.004947		0.0262521	2.967396	0.003930
3rd	**0.5 A**	0.0244341	3.092214	0.007391	**2 A**	0.0211401	2.967396	0.006807
1st		0.0096390	2.239048	0.009639		0.007515	5.910912	0.007515
5th		0.0274572	2.916514	0.003067		0.026154	3.248013	0.002610
3rd	**1 A**	0.0216198	2.850127	0.007539	**2.5 A**	0.0212184	2.735680	0.007803
1st		0.0082755	3.772151	0.008276		0.0072639	6.613072	0.007264

Table 11 Maximum response for model N2

Floor	Current	Displacement	Acceleration	Inter-story	Current	Displacement	Acceleration	Inter-story
5th		0.042499	3.478208	0.004317		0.022932	3.861192	0.002754
3rd	**0 A**	0.033911	3.464131	0.009860	**1.5 A**	0.017448	6.078634	0.005157
1st		0.01422	1.631603	0.014220		0.007149	4.73572	0.007149
5th		0.031226	3.245809	0.005028		0.025469	4.786031	0.004887
3rd	**0.5 A**	0.024395	3.336926	0.007153	**2 A**	0.018229	7.198000	0.005291
1st		0.010076	2.385708	0.010076		0.007637	5.365226	0.007637
5th		0.026059	3.421847	0.003221		0.025741	5.150111	0.002953
3rd	**1 A**	0.019894	4.713008	0.006676	**2.5 A**	0.020111	7.886781	0.006458
1st		0.00817	3.576999	0.008170		0.008877	6.085215	0.008877

Table 12 Maximum response for model N3

Floor	Current	Displacement	Acceleration	Inter-story	Current	Displacement	Acceleration	Inter-story
5th		0.042712	3.520941	0.004290		0.016618	2.078615	0.002149
3rd	**0 A**	0.034179	3.469345	0.009917	**1.5 A**	0.012337	6.573406	0.003758
1st		0.014375	1.65239	0.014375		0.004832	5.270321	0.004832
5th		0.029543	2.913993	0.004594		0.013512	1.933564	0.002661
3rd	**0.5 A**	0.023426	3.876173	0.00692	**2 A**	0.009525	7.499001	0.002839
1st		0.00957	2.397314	0.009570		0.003843	6.194682	0.003843
5th		0.021364	2.362193	0.002538		0.011307	1.991223	0.001173
3rd	**1 A**	0.016517	5.423101	0.005569	**2.5 A**	0.009083	8.605639	0.003173
1st		0.006728	3.982309	0.006728		0.003465	7.047275	0.003465

Table 13 Maximum response for model N4

Floor	Current	Displacement	Acceleration	Inter-story	Current	Displacement	Acceleration	Inter-story
5th		0.043059	3.543355	0.004292		0.021832	2.429627	0.001328
3rd	**0 A**	0.034523	3.548953	0.010029	**1.5 A**	0.019202	8.535859	0.006340
1st		0.014496	1.654527	0.014496		0.006538	5.228568	0.006538
5th		0.030734	3.265234	0.004327		0.0197	2.236319	0.001975
3rd	**0.5 A**	0.02533	5.404789	0.007638	**2 A**	0.017932	10.09289	0.006182
1st		0.010042	2.399432	0.010042		0.00556	6.305119	0.005560
5th		0.025306	2.639537	0.002069		0.0197	2.236319	0.000997
3rd	**1 A**	0.021449	7.315524	0.007599	**2.5 A**	0.017932	10.09289	0.006867
1st		0.007957	4.069022	0.007957		0.00556	6.305119	0.005560

4. Results and discussions

The performance of framed structure subjected to 10 different earthquake motions for various configuration and input currents are assessed and optimal placement of single damper and sequential placement of another damper are obtained. For brevity, only the average response of all considered ground motions is demonstrated in this section.

***For Model Type M*:**

The maximum responses of displacement and acceleration for Model-M (where only one MR damper is placed) are compared in Fig. 5. It is inferred from all the performance indices that damper located in the ground story is best in effectively reducing the overall response of a structure subjected to earthquake excitation. The reduction of inter-story drift for damper placed in ground floor is about 38% and reduction in acceleration response is about 20%. In case of placement of damper at top story the reduction in inter-story drift is only mere 6% and there is a considerable increase in the acceleration response. Therefore, model configuration M1 indicates the optimal placement of a single damper provided in a multi-story structure. Also corresponding to model M1 the fail-safe value for current in case of a feedback failure should be set between 1A - 1.5 A for effective passive control.

***For Model Type N*:**

The peak displacement and acceleration responses for Model-N (where two MR dampers are utilized) are compared in Fig. 6. The reduction of inter-story drift for model ***N3*** is about 75% and reduction in acceleration response is about 48%. However, the reduction in acceleration response in model N2 is maximum of 62% but the corresponding drift reduction is not comparable to model N3. Therefore, the configuration of model N3 is best placement of two MR damper provided in the structure. For two damper configurations, the minimum fail safe value for input current of MR damper at the ground floor should be set at 1 A and that of MR damper in the 2nd floor should be set at 0.5 A to obtain maximum reduction in overall response of a structure.

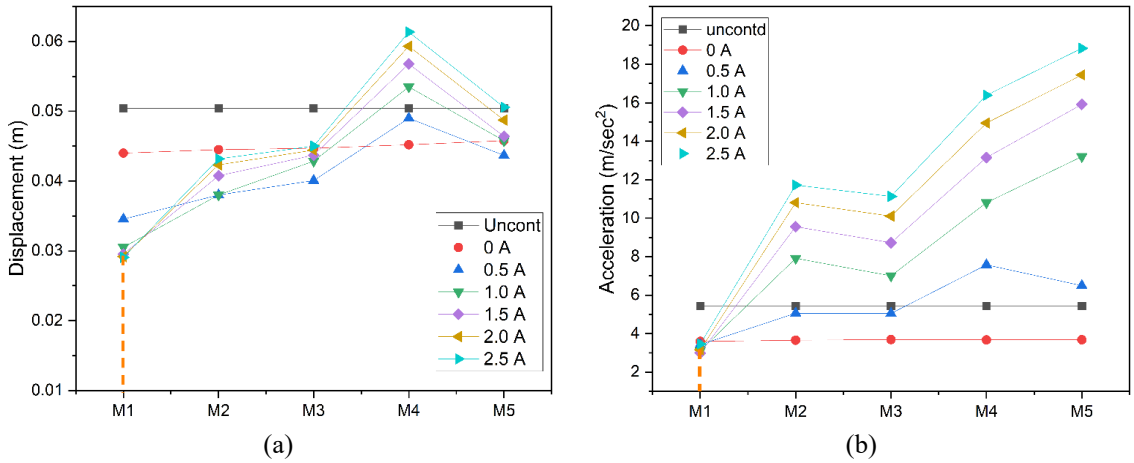

Fig. 5 Peak (a) displacement; and (b) acceleration response of M-type models for all passive strategies

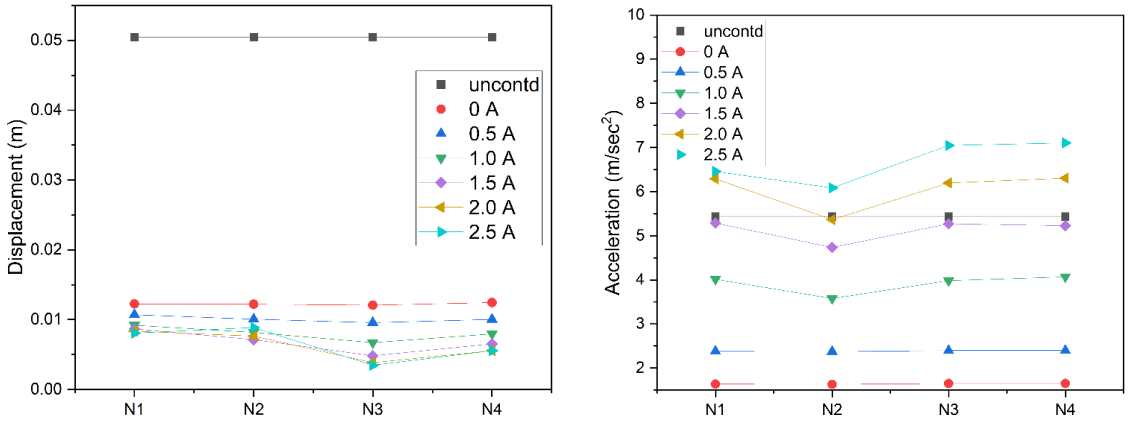

(a) (b)

Fig. 6 Peak (a) displacement and (b) acceleration response of N-type models for all passive strategies

5. Conclusions

This present study is done to investigate the influence of the number, placement and input current of MR dampers on response attenuation of a five-story framed structure subjected to 10 different ground motions ground motion. Also, the response obtained from passive controlled models are compared with the response of uncontrolled structure. The novelty of the study is determination of optimal configuration of MR damper and corresponding passive condition (constant input current) that should be available to the damper as a fail-safe condition This investigation has led to the following deductions:

(1) The number and placement of MR dampers along the structure's height have a significant impact on the structural response. For all stories in this building, the placement of two dampers resulted in higher performance than a single damper.
(2) When only single damper is used it should be placed in the ground story in order to obtain maximum reduction in displacement, acceleration and overall drift reduction. A minimum fail-safe value for input current for single damper configuration should be between I/4 and I/2 (I is the maximum input current) as there isn't much reduction in displacement and inter-story drift but much increase in the absolute floor acceleration for higher values of input current.
(3) When two dampers are used the best configuration to reduce the floor displacement and inter-story drift is to place one damper in the ground floor and other in the 2nd floor (Model N3) and maximum reduction in absolute floor acceleration is obtained for Model N2. For two damper configurations the minimum fail safe value for input current of MR damper at the ground floor should be set at I/2 and that of MR damper in the 2nd floor should be set at I/4 to obtain maximum reduction in overall response of a structure.
(4) The distribution of more than two MR dampers in a structure should be performed by placing one damper in each story starting from the ground floor then the 2nd followed by 1st and rest of the floors sequentially

Acknowledgments

The authors would like to express thanks to the Civil Engineering Department and Electrical Engineering Department of the National Institute of Technology Srinagar, India, for providing support to conduct the work associated with this study.

Conflict of interest

All authors declare that there is no conflict of interest.

References

Abdullah, M.M., Richardson, A. and Hanif, J. (2001), "Placement of sensors/actuators on civil structures using genetic algorithms", *Earthq. Eng. Struct. Dyn.*, **30**(8), 1167-1184. https://doi.org/10.1002/eqe.57

Agarwal, P.K., Sharir, M. and Sharir, M. (1998), "Efficient algorithms for geometric optimization", *ACM Computing Surveys* (*CSUR*), **30**(4), 412-458. https://doi.org/10.1145/299917.299918

Aydin, E., Farsangi, E.N., Öztürk, B., Bogdanovic, A. and Dutkiewicz, M. (2019a), "Improvement of building resilience by viscous dampers", *Resil. Struct. Infrastruct.*, pp. 105-127 https://doi.org/10.1007/978-981-13-7446-3_4

Aydin, E., Öztürk, B. and Dutkiewicz, M. (2019b), "Analysis of efficiency of passive dampers in multistorey buildings", *JSV*, 439, pp. 17-28. https://doi.org/10.1016/J.JSV.2018.09.031

Basu, B., Bursi, O.S., Casciati, F., Casciati, S., Del Grosso, A.E., Domaneschi, M., Faravelli, L., Holnicki-Szulc, J., Irschik, H., Krommer, M. and Lepidi, M. (2014), "A European Association for the Control of Structures joint perspective. Recent studies in civil structural control across Europe", *Struct. Control Health Monitor.*, **21**(12), 1414-1436. https://doi.org/10.1002/STC.1652

Berasategui, J., Elejabarrieta, M.J. and Bou-Ali, M.M. (2014), "Characterization analysis of a MR damper", *Smart Mater. Struct.*, **23**(4), 045025. https://doi.org/10.1088/0964-1726/23/4/045025

Çeşmeci, Ş. and Engin, T. (2010), "Modeling and testing of a field-controllable magnetorheological fluid damper", *Int. J. Mech. Sci.*, **52**(8), 1036-1046. https://doi.org/10.1016/j.ijmecsci.2010.04.007

Cetin, H., Aydin, E. and Ozturk, B. (2019), "Optimal design and distribution of viscous dampers for shear building structures under seismic excitations", *Front. Built Environ.*, 5, p. 90. https://doi.org/10.3389/FBUIL.2019.00090

Chaudhury, D. and Singh, Y. (2014), "Performance-based design of RC frame buildings with metallic and friction dampers", *J. Inst. Engr. (India): Series A*, **95**(4), 239-247. https://doi.org/10.1007/s40030-014-0089-4

Chen, C., Ricles, J.M., Sause, R. and Christenson, R. (2010), "Experimental evaluation of an adaptive inverse compensation technique for real-time simulation of a large-scale magnetorheological fluid damper", *Smart Mater. Struct.*, **19**(2), 025017. https://doi.org/10.1088/0964-1726/19/2/025017

Chen, B., Wu, J., Ouyang, Y. and Yang, D. (2018), "Response evaluation and vibration control of a transmission tower-line system in mountain areas subjected to cable rupture", *Struct. Monitor. Maint., Int. J.*, **5**(1), 151-171. https://doi.org/10.12989/smm.2018.5.1.151

Cimellaro, G.P. (2012), "Optimal placement of controller for seismic structures", In: *Design Optimization of Active and Passive Structural Control Systems*, pp. 1-33. https://doi.org/10.4018/978-1-4666-2029-2.ch001

De Vicente, J., Klingenberg, D.J. and Hidalgo-Alvarez, R. (2011), "Magnetorheological fluids: A review", *Soft Matter*, **7**(8), 3701-3710. https://doi.org/10.1039/c0sm01221a

Dhingra, A.K. and Lee, B.H. (1994), "Optimal placement of actuators in actively controlled structures", *Eng.*

Optimiz., **23**(2), 99-118. https://doi.org/10.1080/03052159408941347
Guan, X.C., Guo, P.F. and Ou, J.P. (2011), "Modeling and analyzing of hysteresis behavior of magneto rheological dampers", *Procedia Eng*., **14**, 2756-2764. https://doi.org/10.1016/j.proeng.2011.07.347
Hagood, N.W., Chung, W.H. and Von Flotow, A. (1990), "Modelling of piezoelectric actuator dynamics for active structural control", *J. Intell. Mater. Syst. Struct*., **1**(3), 327-354. https://doi.org/10.1177/1045389X9000100305
He, X.Y., Li, H.N. and Zhang, J. (2016a), "Multi-dimensional seismic response control of offshore platform structures with viscoelastic dampers (I-Theoretical analysis)", *Struct. Monitor. Maint*., *Int. J*., **3**(2), 157-174. https://doi.org/10.12989/smm.2016.3.2.157
He, X.Y., Zhao, T.W., Li, H.N. and Zhang, J. (2016b), "Multi-dimensional seismic response control of offshore platform structures with viscoelastic dampers (II-Experimental study)", *Struct. Monitor. Maint*., *Int. J*., **3**(2), 175-194. https://doi.org/10.12989/smm.2016.3.2.175
Hong, S.R., Wereley, N.M., Choi, Y.T. and Choi, S.B. (2008), "Analytical and experimental validation of a nondimensional Bingham model for mixed-mode magnetorheological dampers", *J. Sound Vib*., **312**(3), 399-417. https://doi.org/10.1016/j.jsv.2007.07.087
Ibidapo-Obe, O. (1985), "Optimal actuators placements for the active control of flexible structures", *J. Mathe. Anal. Applicat*., **105**(1), 12-25. https://doi.org/10.1016/0022-247X(85)90094-0
Jolly, M.R., Bender, J.W. and Carlson, J.D. (1999), "Properties and applications of commercial magnetorheological fluids", *J. Intell. Mater. Syst. Struct*., **10**(1), 5-13. https://doi.org/10.1177/1045389x9901000102
Korkmaz, S. (2011), "A review of active structural control: Challenges for engineering informatics", *Comput. Struct*., **89**(23-24), 2113-2132. https://doi.org/10.1016/j.compstruc.2011.07.010
Lindberg Jr, R.E. and Longman, R.W. (1984), "On the number and placement of actuators for independent modal space control", *J. Guid. Control Dyn*., **7**(2), 215-221. https://doi.org/10.2514/3.56366
Nabid, N., Hajirasouliha, I. and Petkovski, M. (2019), "Adaptive low computational cost optimisation method for performance-based seismic design of friction dampers", *Eng. Struct*., **198**, p. 109549. https://doi.org/10.1016/j.engstruct.2019.109549
PEER, P.E.E.R. Center (2013), PEER Ground Motion Database, Shallow Crustal Earthquakes in Active Tectonic Regimes, NGA-West2.
Preumont, A. (2011), *Vibration Control of Active Structures*, Springer. https://doi.org/10.1007/978-94-007-2033-6_1
Qiu, Z.C., Zhang, X.M., Wu, H.X. and Zhang, H.H. (2007), "Optimal placement and active vibration control for piezoelectric smart flexible cantilever plate", *J. Sound Vib*., **301**(3-5), 521-543. https://doi.org/10.1016/j.jsv.2006.10.018
Singh, M.P. and Moreschi, L.M. (2002), "Optimal placement of dampers for passive response control", *Earthq. Eng. Struct. Dyn*., **31**(4), 955-976. https://doi.org/10.1002/eqe.132
Spaggiari, A. (2012), "Properties and applications of magnetorheological fluids", *Frattura ed Integrita Strutturale*, **7**(23), 48-61. https://doi.org/10.3221/IGF-ESIS.23.06
Spencer Jr, B.F. and Nagarajaiah, S. (2003), "State of the art of structural control", *J. Struct. Eng*., **129**(7), 845-856. https://doi.org/10.1061/(ASCE)0733-9445(2003)129:7(845)
Stanway, R. (2004), "Vibration Control of Active Structures — An Introduction", *Proceedings of the Institution of Mechanical Engineers*, *Part I*: *Journal of Systems and Control Engineering*. https://doi.org/10.1177/095965180421800308
Wani, Z.R. and Tantray, M.A. (2020), "Parametric Study of Damping Characteristics of Magneto-Rheological Damper: Mathematical and Experimental Approach", *Pollack Periodica Pollack*, **15**(3), 37-48. https://doi.org/10.1556/606.2020.15.3.4
Wani, Z. R. and Tantray, M. (2021), "Study on integrated response-based adaptive strategies for control and placement optimization of multiple magnetorheological dampers-controlled structure under seismic excitations", *J. Vib. Control*, p. 10775463211000484. https://doi.org/10.1177/10775463211000483
Xu, Y.L. and Teng, J. (2002), "Optimum design of active/passive control devices for tall buildings under earthquake excitation", *Struct. Des. Tall Build*., **15**(3), 37-48. https://doi.org/10.1002/tal.193

Xu, Z.D., Guo, Y.Q., Zhu, J.T. and Xu, F.H. (2016), *Intelligent Vibration Control in Civil Engineering Structures*, Intelligent Vibration Control in Civil Engineering Structures. https://doi.org/10.1016/c2012-0-00334-1

Yanik, A. (2020), "Seismic control performance indices for magnetorheological dampers considering simple soil-structure interaction", *Soil Dyn. Earthq. Eng.*, **129**, 105964. https://doi.org/10.1016/j.soildyn.2019.105964

Yoshida, O. and Dyke, S.J. (2005), "Response control of full-scale irregular buildings using magnetorheological dampers", *J. Struct. Eng.*, **131**(5), 734-742. https://doi.org/10.1061/(ASCE)0733-9445(2005)131:5(734)

Zhang, D., Pan, P. and Zeng, Y. (2018), "An optimum model reference adaptive control algorithm for smart ase-isolated structures", *Bull. Earthq. Eng.*, **16**(11), 5647-5610. https://doi.org/10.1007/s10518-018-0403-z

Zhou, H., Xiang, N., Huang, X., Sun, L., Xing, F. and Zhou, R. (2018), "Full-scale test of dampers for stay cable vibration mitigation and improvement measures", *Struct. Monitor. Maint., Int. J.*, **5**(4), 489-506. https://doi.org/10.12989/smm.2018.5.4.489

HL